

**\*\*FULL TITLE\*\***

*ASP Conference Series*, Vol. **\*\*VOLUME\*\***, **\*\*YEAR OF PUBLICATION\*\***

**\*\*NAMES OF EDITORS\*\***

## *Spitzer* Observations of Powerful Radio Sources

K. Cleary<sup>1</sup>, C. R. Lawrence<sup>1</sup>, J. A. Marshall<sup>2</sup>, L. Hao<sup>2</sup> and D. Meier<sup>1</sup>

<sup>1</sup> *Jet Propulsion Laboratory, California Institute of Technology*

<sup>2</sup> *Astronomy department, Cornell University, Ithaca, NY 14853*

**Abstract.** We have measured the mid-infrared radiation from an orientation-unbiased sample of 3C RR galaxies and quasars with  $0.4 < z < 1.2$  using the IRS and MIPS instruments aboard the *Spitzer Space Telescope*. We fit the *Spitzer* data as well as other measurements from the literature with synchrotron and dust components. At  $15\,\mu\text{m}$ , quasars are typically four times brighter than radio galaxies with the same isotropic radio power. Based on our fits, half of this difference can be attributed to the presence of non-thermal emission in the quasars but not the radio galaxies. The other half is consistent with dust absorption in the radio galaxies but not the quasars.

### 1. Introduction

Only a small fraction of AGN produces the prodigious radio power of FR II galaxies and quasars. Nevertheless, the fact that FRIIs can be studied in an orientation-unbiased sample, selected on the basis of low-frequency radio emission, makes them uniquely valuable in separating the effects of orientation from physical differences. The mid- and far-infrared properties of these powerful radio sources are largely unknown. Their space density is so low that only a few (e.g., 3C 405 = Cygnus A) are at low redshifts. The *Spitzer Space Telescope* (Werner et al. 2004) promised a major advance in sensitivity over previous telescopes, and the capability to measure these objects. We therefore undertook observations with *Spitzer* of powerful radio sources. The overall goal was straightforward: to measure for the first time the mid- and far-infrared emission from an orientation-unbiased sample of the powerful radio sources.

This paper gives a brief overview of the observations, data reduction and some of the main results. Further details may be found in Cleary et al. (2007).

### 2. The Sample

We require a sample selected at low frequency, with  $L_{178\text{MHz}} > 10^{26}\text{ W Hz}^{-1}\text{ sr}^{-1}$  and with a reasonable balance between FR II radio galaxies and quasars.

The sample of Barthel (1989) provides the ideal starting point. It contains the 50 sources in the complete low-frequency 3C RR catalog of Laing et al. (1983) with  $0.5 \leq z \leq 1.0$ . All have emitted radio luminosity  $L_{178\text{MHz}} > 10^{26}\text{ W Hz}^{-1}\text{ sr}^{-1}$ . To reduce the observing time required, we reduced the sample to 33 objects based on ecliptic latitude. We also added one source to the sample,

3C 200, at  $z = 0.458$ , because we already had a 16 ks *Chandra* observation of it. The *Spitzer* sample consists of 16 quasars and 18 galaxies.

### 3. Observations and Data Reduction

All sources in the sample were scheduled for observation with the Long-Low module of the *Spitzer* Infrared Spectrograph (IRS; Houck et al. 2004) resulting in spectra in the range  $15\text{--}37\text{ }\mu\text{m}$ , as well as with the Multiband Imaging Photometer (MIPS; Rieke et al. 2004) in photometry mode at  $24$ ,  $70$ , and  $160\text{ }\mu\text{m}$ . All objects in the sample are unresolved by the *Spitzer* instruments.

The IRS spectra were extracted from the basic calibrated data (BCD) images provided by the Spitzer Science Center, using the Spectroscopy Modeling and Analysis Tool (SMART; Higdon et al. 2004). Mosaics of the MIPS  $24$  and  $70\text{ }\mu\text{m}$  BCD images were produced using the Mosaicking and Point Source Extraction tool, MOPEX (Makovoz & Khan 2005), while for  $160\text{ }\mu\text{m}$ , the post-BCD mosaics provided by the SSC were used.

### 4. Spectral Fitting

We fit the IRS and MIPS data, as well as additional photometry from the NED, with models for the thermal and non-thermal emission, in order to separate their respective contributions to the mid-infrared. Simple functional forms are used to model the lobe and jet synchrotron components, while the warm dust component is modeled as an optically thin spherical shell of graphite and silicate grains surrounding a source with an AGN accretion disk spectral energy distribution. We also allow for the possibility that the dust component is partially obscured behind a screen of cooler dust.

For all of the objects in the sample with IRS spectra, we performed fits to the SED using the following combinations of components:

- warm dust + lobe synchrotron;
- warm dust + lobe synchrotron + jet synchrotron;
- warm dust + lobe synchrotron + cool dust;
- warm dust + cool dust + lobe synchrotron + jet synchrotron,

with the free parameters varying simultaneously. In general, the combination of components which resulted in the best reduced chi-squared was selected as the best fit. Figure 1 shows the best fits for the quasar 3C 138 and the galaxy 3C 340.

### 5. Results

We detect powerful emission in the mid-infrared for our sample of radio galaxies and quasars. All objects in our sample except one were detected at  $24\text{ }\mu\text{m}$  using MIPS, with luminosities  $L_{24\text{ }\mu\text{m}} > 10^{22.4}\text{ W Hz}^{-1}\text{ sr}^{-1}$ . In the discussion below, we characterize the infrared luminosities at rest-frame wavelengths of  $15$  and  $30\text{ }\mu\text{m}$  using the IRS and MIPS measurements.

### 5.1. Non-thermal Contribution

Synchrotron emission from optically thin radio lobes has flux-density spectral indices  $\alpha \approx -0.7$ , so the contribution to the infrared is typically well over an order of magnitude below the observed flux density. However, Doppler-boosted synchrotron emission from dense, compact regions is a potentially serious contaminant of the infrared emission. The relative contribution of thermal and non-thermal processes to the infrared emission of AGN has been the subject of many studies.

The *Spitzer* observations described here have provided further constraints on the role of non-thermal processes in the infrared emission of radio galaxies and quasars. In §4, we fitted the SEDs of the objects in our sample with broadband spectral components representing synchrotron emission from the radio lobes and jet as well as thermal emission from circumnuclear dust (see Fig. 1). In this way, the non-thermal contribution to the 15 and 30  $\mu\text{m}$  luminosity was estimated and subtracted from the observed emission. For the galaxies, the thermal contribution is always  $> 80\%$ ; for the quasars, the thermal contribution is in the range 10–100%. All objects, quasars and galaxies, were fitted in a consistent manner; however, it is only the quasars in the sample which were estimated to have a non-thermal contribution  $> 20\%$ .

### 5.2. Comparative Luminosity of 3C RR Radio Galaxies and Quasars

In order to compare the infrared luminosities of quasars and radio galaxies we must first account for the variation of central engine power amongst objects in our sample. To do this, we normalize the infrared emission by the isotropic low-frequency radio luminosity to get  $R_{\text{dr}} = \nu L_{\nu}(\text{IR})/\nu L_{\nu}(178 \text{ MHz})$ .

The mean  $R_{\text{dr}}$  for quasars is  $\sim 4$  times higher than for galaxies at 15  $\mu\text{m}$ . Subtracting the non-thermal emission brings this down to  $\sim 2$ . The fitted optical depths allow us to go further and ask whether obscuration by dust can account for this residual anisotropy of the thermal emission between quasars and galaxies. Using the fitted screen optical depths to correct for dust extinction, we find that the thermal emission from quasars and galaxies is on average equal at 15  $\mu\text{m}$ .

Figure 2 plots the screen optical depths,  $\tau_{9.7\mu\text{m}}^{\text{scr}}$ , against the core dominance parameter,  $R = F_{\text{core}}/F_{\text{extended}}$ . Our dust model (see §4) does not, a priori, impose any asymmetry in the distribution of dust surrounding the nucleus. From Figure 2 there is evidence of an anti-correlation between optical depth and core dominance, from which we can infer an equatorial distribution of dust. The median screen (mixed) optical depth for objects with  $R > 10^{-2}$  is 0.4 (1.0) and with  $R \leq 10^{-2}$  is 1.1 (3.0).

## 6. Conclusions

It is clear from previous work that beamed synchrotron emission and dust extinction modulate the mid-infrared emission of quasars and radio galaxies to some degree. In the work presented here, however, we have quantified these effects for an orientation-unbiased sample of powerful radio sources and shown that once they are taken into account, quasars and radio galaxies are on average equally bright in the mid-infrared.

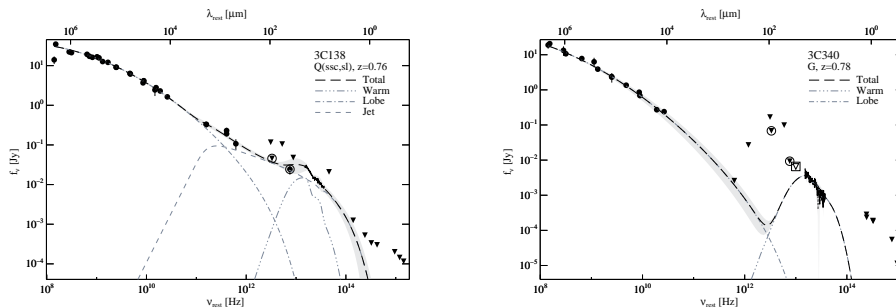


Figure 1. The fits to the IRS spectra and photometric data for the quasar 3C138 (left) and galaxy 3C340 (right) are shown as examples. Filled circles and triangles represent detections and upper limits, respectively. Symbols within circles represent the MIPS measurements.

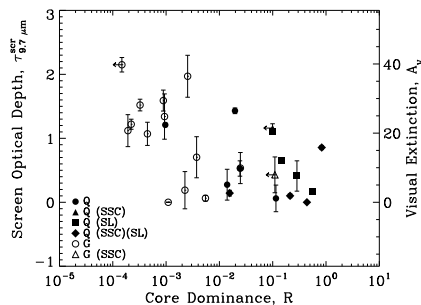


Figure 2. The  $9.7 \mu\text{m}$  screen optical depths estimated from the fits to the data versus the core dominance parameter,  $R = F_{\text{core}}/F_{\text{extended}}$ . The right-hand  $y$ -axis indicates the visual extinction. From the apparent anti-correlation of optical depth with core dominance, we infer an equatorial distribution of cool dust consistent with the “dusty torus” of orientation-based unification schemes.

**Acknowledgments.** The research described in this paper was carried out at the Jet Propulsion Laboratory, California Institute of Technology, under a contract with the National Aeronautics and Space Administration.

## References

- Barthel, P.D. 1989, ApJ, 336, 606
- Cleary, K. et al. 2007, ApJ, 660, 117
- Higdon, S. J. H., et al. 2004, PASP, 116, 975
- Houck, J. R., et al. 2004, ApJS, 154, 18
- Laing, R. A., Riley, J. M., & Longair, M.S. 1983, MNRAS, 204, 151
- Makovoz, D., & Khan, I. 2005, in *Astronomical Data Analysis Software and Systems VI*, ed. P. L. Shopbell, M. C. Britton, & R. Ebert (San Francisco: ASP), 81
- Rieke, G. H., et al. 2004, ApJS, 154, 25
- Werner, M. W., et al. 2004, ApJS, 154, 1